Circulation types related to lightning activity over Catalonia and the Principality of Andorra

N. Pineda [a], P. Esteban [b,c,*], L. Trapero [b], X. Soler [a,c], C. Beck [d]

[a] Meteorological Service of Catalonia (SMC), Berlín 38, Barcelona E-08029, Catalonia, Spain
[b] Snow and Mountain Research Centre of Andorra - Institut d'Estudis Andorrans (CENMA/IEA), Avda. Rocafort 21-23 Edifici Molí, Sant Julià de Lòria AD600, Andorra
[c] Group of Climatology – University of Barcelona, Laboratori de Climatologia, Montalegre 6, Barcelona E-08001, Catalonia, Spain
[d] Institute of Geography, University of Augsburg, Universitaetsstrasse 10 Augsburg D-86135, Germany

1. Introduction and objectives

Circulation-type classifications have been applied to different spatial and temporal scales and atmospheric variables. Recently, due to the improvement of weather-station networks and the availability of gridded circulation data (NCEP/NCAR Reanalysis, ERA40 database, etc.), many authors are dealing with the daily scale in an attempt to further our knowledge of extreme events such as heavy precipitation, local phenomena like air pollution, or other weather- and climate-related impacts on society. As is well-known, establishing statistical relationships between the synoptic and the local scale, clearly improves the interpretation and conclusions that can be obtained from General Circulation Models (GCM) in the evaluation of climate change, due to the fact that they attempt to solve limitations referring to the spatial resolution of the dynamical models. Furthermore, weather forecasting applications (among others) can also be derived from these statistical techniques (Huth et al., 2008). Thus, the main objective of the Action COST-733 (2009) on Harmonisation and applications of weather type Classifications for European Regions (http://www.cost733.org/) is to "achieve (a) general numerical method(s) for assessing, comparing and classifying weather situations in Europe, scalable to any European (sub) region with time scales between 12 h and 3 days and spatial scales of ca. 200–2000 km, applicable for a number of applications". Methods such as ones based on correlations, Principal Components Analysis, Clustering Techniques or Neural Networks are being tested in this European project. See Huth et al. (2008) and Philipp et al. (2010) for an extensive review of these methods and applications.

Reap (1994) pointed out that circulation types can be used to analyse typical weather patterns related with thunderstorms, as well as the spatial distribution of lightning activity. Moreover, climatological studies on lightning can be useful in operational

* Corresponding author. Address: Snow and Mountain Research Centre of Andorra - Institut d'Estudis Andorrans (CENMA/IEA), Avda. Rocafort 21-23 Edifici Molí, Sant Julià de Lòria AD600, Andorra. Tel.: +376 742630.
E-mail address: pesteban.cenma@iea.ad (P. Esteban).

settings, as they can be used to develop probability equations for predicting thunderstorm distributions associated with the major flow patterns (Lericos et al., 2002). Several researchers have analyzed lightning distributions as a function of the prevailing large-scale flow over different regions in the world. For example, over central Florida (US), López and Holle (1987) showed its dependence on the prevailing low-level flow, and Lericos et al. (2002) have found that some flow patterns were more conducive to cloud-to-ground (CG) flashes than others. In Europe, Hagen and Finke (1999) have related the probability of thunderstorms in Germany to weather patterns based on a low-level flow classification. In Spain, Tomás et al. (2004) have found that convective processes can be associated with a small number of general synoptic situations obtained with the Jenkinson and Collison (1977) classification method. Following these analysis of lightning distributions as a function of the atmospheric circulation type, the aim of this paper is to improve our knowledge of thunderstorm activity, from the dynamical and statistical point of view, over Catalonia and the Principality of Andorra. This objective will be achieved through a classification of atmospheric circulation types associated with substantial lightning activity in 6-h periods, in order to obtain the main Sea Level Pressure (SLP) types and associated information such as: monthly and 6-h frequencies, sequence types, and lightning activity spatial distribution. Furthermore, for weather forecasting purposes, we analyzed some meteorological variables and indexes, and calculated the frequencies of occurrence of substantial lightning activity for SLP configurations showing a high degree of similarity to the centroid patterns of the circulation types.

A feature that must be considered for the analysis is the particular orography of the study area: the coastline oriented from northeast to southwest with two mountain ranges of around 1000 m altitude running roughly parallel to it, delimited by the Pyrenees (with maximums heights of 3000 m and where Andorra is located) to the North and the Ebro river valley to the West (Fig. 1). Air flows are highly influenced by these orographic features and their direction and speed can be modified. Some important effects are: blockage of the air flow by mountain barriers or generation of channelling winds through river valleys and consequently the presence of convergence areas inland.

2. Data and methods

2.1. Lightning data

Lightning information was collected by a SAFIR lightning detection system (Richard and Lojou, 1996) operated by the Meteorological Service of Catalonia (SMC). Three sensors, covering the region of Catalonia and its contiguous areas, including the Principality of Andorra, make up the network (Fig. 1). The SAFIR system combines interferometry (in the very high frequency, VHF) for detecting intra-cloud flashes (IC) with direction finding (Low Frequency, LF) for discriminating cloud-to-ground flashes (CG). The SMC–SAFIR system presents a detection efficiency of around 90% and a lightning localization accuracy of approximately 2–3 km (Pineda and Montanyà, 2009). We grouped the lightning activity of the 5 years analyzed (2003–2007), into 6-h periods, according to four daily NCEP analyses hours (00 h-06 h-12 h-18 h UTC). Thus, the 6-h periods are from 21 h to 03 h, from 03 h to 09 h, etc. We only analyzed the 6-h periods with over 200 CG, which provided a sample of more than 460 6-h periods covering 82% of the CG flash counts recorded in Catalonia and Andorra from January 2003 to December 2007.

2.2. Numerical model data

The gridded data used for classification of the circulation types is the NCEP Final Analyses of the Global Tropospheric Analyses (NCEP FNL data; FNLDOC/NOAA/NWS/NCEP, 2000) at 1° resolution over the region 35°N–48°N by 5°W–8°E. The meteorological field classified is Sea Level Pressure (SLP).

2.3. Circulation type classification

The classification method used in this study is the one presented by Esteban et al. (2005, 2006, 2009) based on Principal Component Analysis (PCA) with the "extreme scores" variant for clustering all the cases. The method follows the well-known S-mode based procedure (Richman, 1986; Yarnal, 1993) with previous deseasonalisation of the data via spatial standardisation (scaling the rows). Additionally, the correlation matrix is used to provide the most efficient representation of variance in the dataset (Barry and Carleton, 2001), and the orthogonal Varimax rotation of Principal Components (PCs) is applied to facilitate the spatial interpretation of the PCs (Yarnal, 1993). The Scree test criterion and the North rule-of-thumb are the methods used for retaining the relevant PCs.

Based on the standardized PC scores, the decision regarding the number of groups (CTs) and the definition of their initial centroids is based upon the principle of "extreme scores". The basic idea of this approach entails using observations exhibiting "extreme scores" on one of the retained and rotated PCs (usually values higher than +2 for the positive phase, lower than −2 for the negative phase) while having low score values on the remaining PCs (usu-

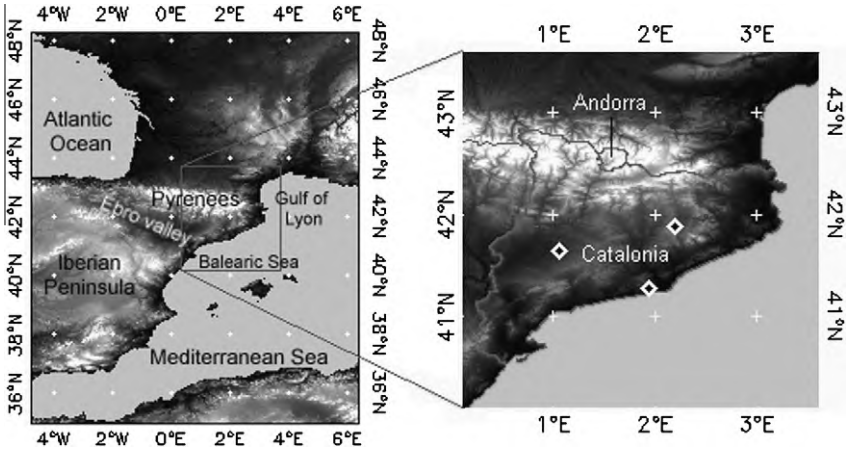

Fig. 1. (a) Area of interest, NE of the Iberian Peninsula. (b) Catalonia and Andorra with the lightning detection sensors (diamonds) of the Meteorological Service of Catalonia (SMC).

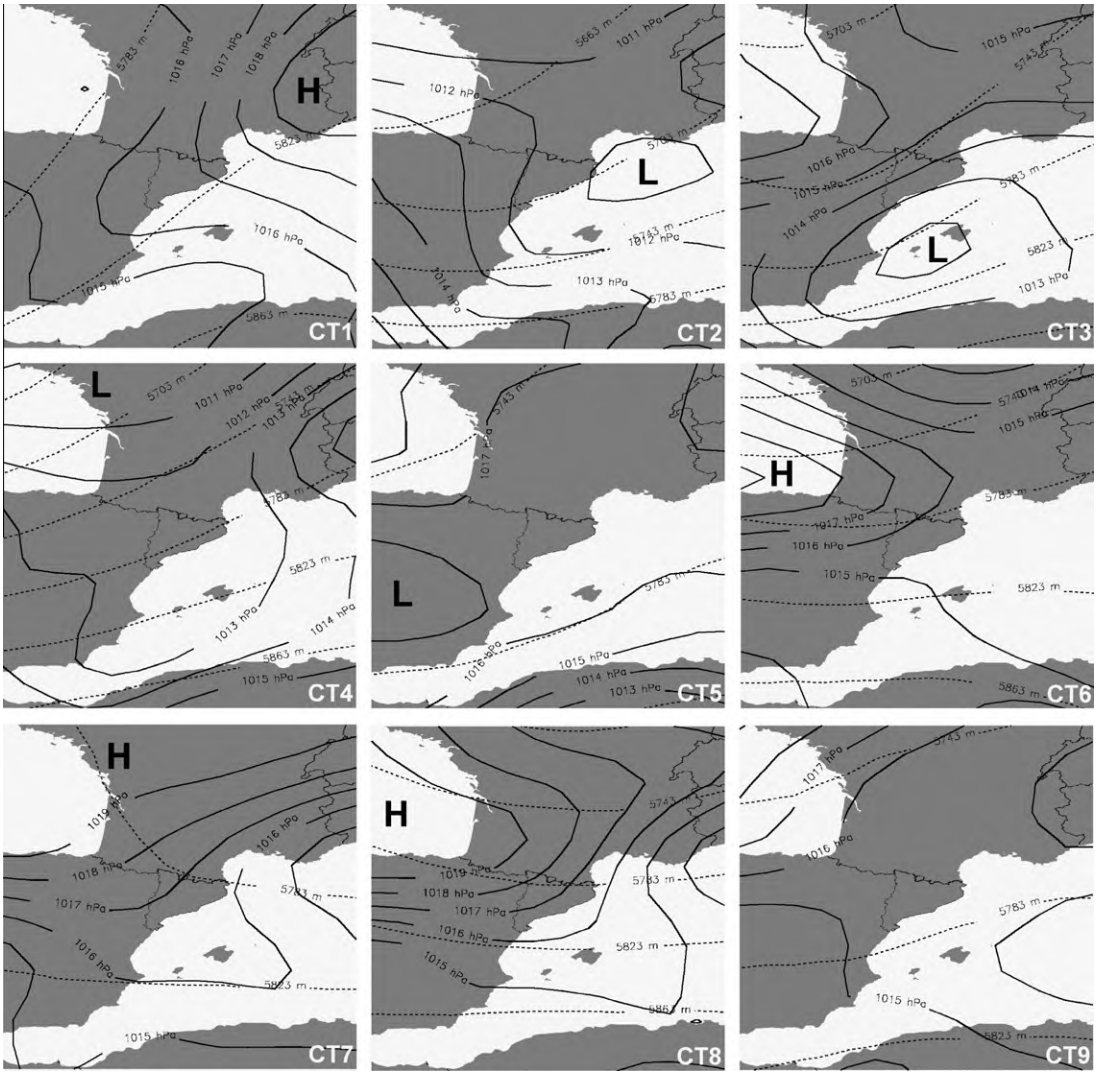

Fig. 2. SLP synoptic circulations types (solid lines) and 500 hPa geopotential heights (dashed lines) based on multivariate techniques (centroids of clusters 1–9 for 6-h periods with a threshold of over 200 cloud-to-ground flashes).

ally values between +1 and −1) for defining the initial centroids of the CTs of the final classification catalogue. Subsequently, these centroids are calculated by averaging all observations that can be assigned to one PC according to "extreme scores" criteria (Tait and Fitzharris, 1998; Birkeland et al., 2001; Kostopoulou, 2003). Normally 2.5–5% of all cases are used to obtain the initial centroids (4.10% for the classification presented in this paper). PCs to which no observation can be assigned (i.e. there is no day with a close spatial structure), are considered as an artificial result from the PCA, and consequently this potential group (circulation type) is eliminated. Thus, this procedure avoids artefacts in the final classification that may result when relying solely on the methods for retaining the main components and the Varimax rotation applied during the preceding PCA. Finally, all observations (6-h lightning periods) are assigned to the nearest initial centroid in terms of the Euclidean distance (calculated with the standardized scores values) for obtaining the definitive CTs. It should be noted that the commonly used *K*-means iterative method was not applied as the last step for classifying all the observations, assuming that the centroids were well-established using the "extreme scores" criterion (the centroids related to the PCs have a spatial structure close to the observed 6-h circulation cases), and no optimisation procedure was required. Details of this method can also be found in Philipp et al. (2010).

3. Results

Nine SLP circulation types (CT) were identified with the above mentioned PCA and clustering method, which are shown in Fig. 2. Additionally, to facilitate the meteorological interpretation, the mean geopotential height at 500 hPa for each CT has been added to the maps. Fig. 3 shows the CT monthly frequencies, the frequencies for 6-h periods and the lightning activity of each pattern. It also shows transition frequencies among CTs between consecutive 6-h periods. Fig. 4 shows the spatial distribution of flashes determined over all the CG activity of the 6-h periods related to each CT.

3.1. CT1: Easterly flow

High pressures over continental Europe, generating Mediterranean winds (east to southeast) over the Catalonian coast and a south-westerly flow at 500 hPa causing significant shear (Fig. 2). The frequencies obtained show evident concentration of this

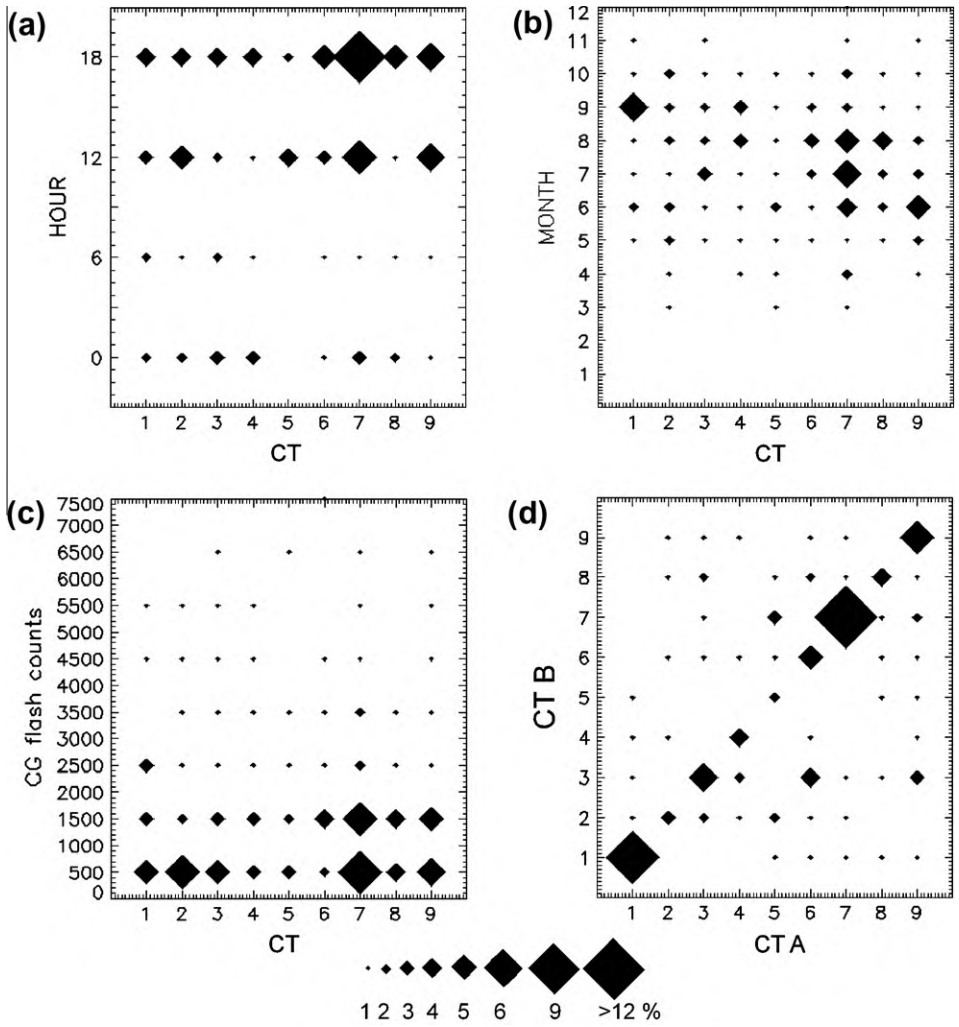

Fig. 3. (a) Six-hourly and (b) monthly frequencies of the clusters obtained, (c) distribution of circulation types (CTs) by cloud-to-ground flashes (CG), and (d) transition frequencies among CTs between consecutive 6-h periods (CT A–CT B).

pattern in September and a homogeneous hourly distribution (Fig. 3). The spatial distribution of flashes related to this circulation type exhibits a major concentration of lightning along the Mediterranean coastline (Fig. 4). This distribution, together with the homogeneous hourly distribution across the day, points to a maritime origin of the thunderstorms. The Mediterranean Sea supplies warm and humid air through onshore flow in the lower troposphere, especially during autumn (the so called "Mediterranean Air Mass" by Jansà (1959)), combined with the advance of a wave trough at 500 hPa. Such conditions can lead to heavy rainfall events, which are frequent on the Catalonian coastline at the beginning of autumn, and which sometimes affect the Pyrenees, depending on the orographic forcing required for instability (Llasat and Puigcerver, 1994).

3.2. CT2: Westerly flow with Mediterranean low

The monthly distribution of this pattern has distinct maximums in the spring and autumn months. This type represents a frontal system coming from the west and crossing the study area. In addition, the arrival of the associated air mass over the Mediterranean could generate a dynamical low, on average centered over the Gulf of Lyon. Spatial lightning distribution for this CT shows a mixture of the typical spring and autumn patterns in the region. As in spring, thunderstorms tend to occur in the Pyrenees and in nearby continental Catalonia; in autumn the activity is located in the Mediterranean Sea and on the Catalonian coastline.

3.3. CT3: Mediterranean low

Dynamical low over the Mediterranean Sea, located on average in the Balearic Sea and pumping humid air over the Catalonian coast. This pattern presents intense lightning activity, mainly during the 6-h periods at 18 h and 00 h UTC. Occurrence thereof, despite the summer maximums, is well distributed over all months with substantial lightning activity in our dataset. The spatial lightning distribution for this CT shows that this Balearic Sea dynamical low generates lightning activity mainly along the Catalonian coast, especially the southern part. The other maximum of activity, located in continental Catalonia, is related to the channelling of the Mediterranean humid air in river valleys and subsequent orographic uplift further inland (mainly on the southern slopes of the Pyrenees).

3.4. CT4: Westerly flow

As in CT2, a frontal system is crossing the area, but in this case with a more pronounced south-westerly component of winds. Frequency maxima appear in August and September and during night time. Thunderstorms usually develop in the west

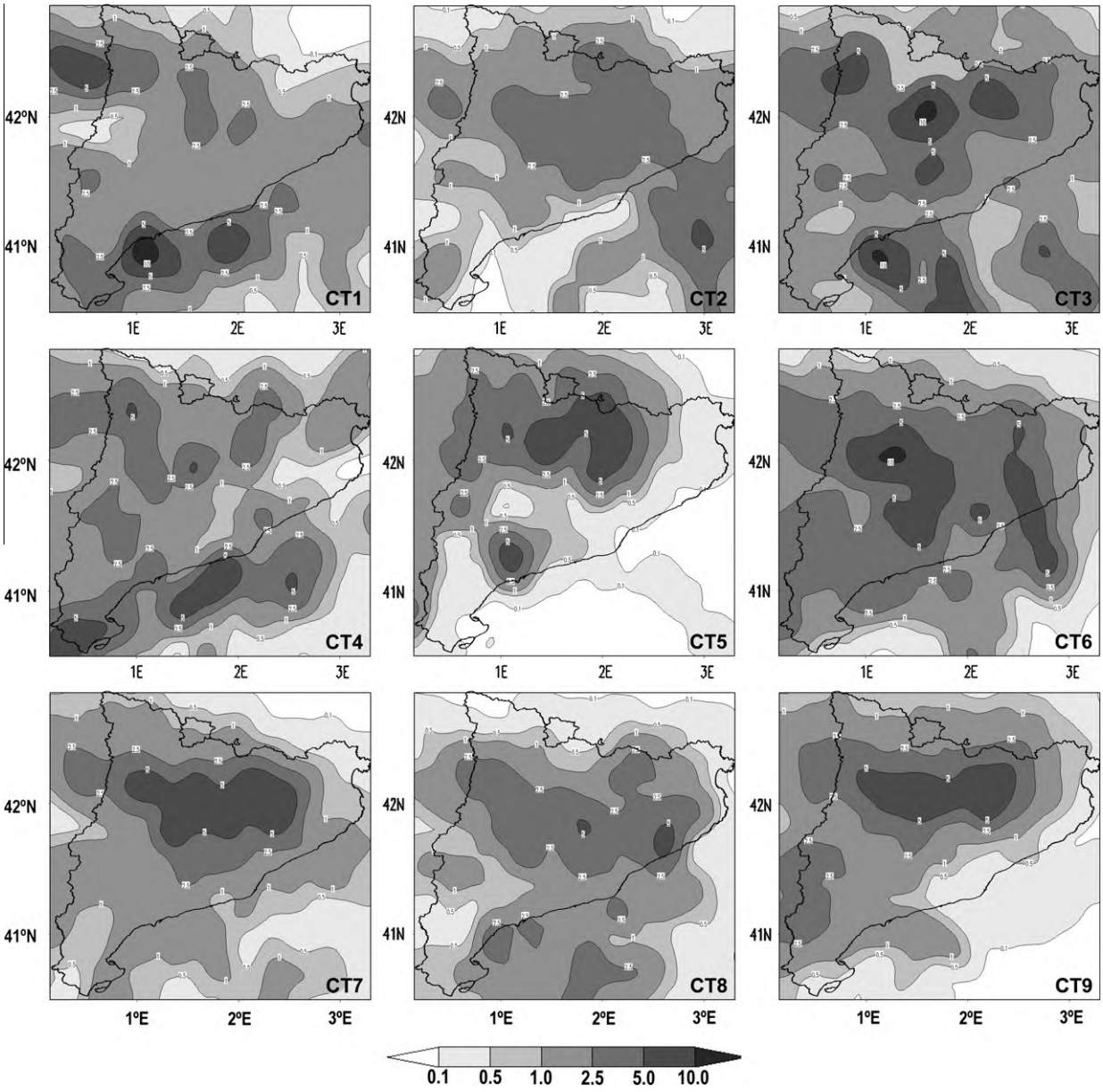

Fig. 4. Spatial lightning distributions over Catalonia and Andorra for each CT. Isolines are calculated after rating the total CG counts of each CT for the number of its corresponding 6 h-periods in a mesh of 0.1°.

of the study area (mainly in Aragon) and reach Catalonia in a mature stage, affecting the inland areas. Subsequently, contact between the frontal system and the Mediterranean Sea, which is warm and humid at the end of summer and autumn, reinforces the convection once again.

3.5. CT5: Iberian thermal low

Low-pressure gradient over the area and presence of a thermal low centered over the Iberia Peninsula. The annual maxima are in late spring and at the beginning of summer. It is interesting to highlight the lack of this type at night and in the morning; this diurnal evolution pattern is clearly related to the solar radiation cycle. The spatial lightning distribution for this CT has a minimum activity over the sea and shows high activity in mountain regions, related to local convection in spring and early summer, when solar heating over the relief generates higher vertical temperature gradients than the free atmosphere. Hence, this CT shows maxim values over Andorra and the topmost areas in the Pyrenees, mainly in its eastern half. This is a well-known circulation pattern over Iberia (Martín-Vide, 2005; Esteban et al., 2006), which is not always sufficiently clearly identified by classification methods.

3.6. CT6: Cold front

Low-pressure systems crossing Europe; the study area is affected by the southern part of the frontal system. Subsequently, the Azores high directs northerly winds over the Pyrenees. Monthly maximum registered in August and daily maxima at the afternoon–evening hours. The spatial lightning distribution for this CT shows thunderstorms affecting almost the whole region from west to east, probably due to the westerly flow at 500 hPa. It is important to highlight that the local maximum in the east is related to one single extreme event.

Table 1
Mean and standard deviation values for temperature difference between 850 and 500 hPa, (TD850-500), CAPE and Lifted Index (LI) for each circulation pattern (CT).

	TD850-500 (°C)	Cape (J/kg)	LI
CT1 – Easterly flow	27.7 (2.1)	365.7 (379.9)	−0.7 (2.2)
CT2 – Westerly flow & Mediterranean low	28.1 (2.2)	236.8 (335.9)	0.4 (2.5)
CT3 – Mediterranean low	27.6 (2.4)	323.7 (397.2)	−0.2 (2.5)
CT4 – Westerly flow	28.9 (2.5)	476.9 (458.2)	−1.1 (2.5)
CT5 – Iberian thermal low	29.0 (2.1)	231.2 (276.3)	0.1 (2.2)
CT6 – Cold front	28.4 (2.0)	378.6 (406.7)	−0.7 (2.7)
CT7 – North-eastern flow	28.4 (2.1)	275.0 (343.7)	0.2 (2.6)
CT8 – Azores anticyclone	26.8 (2.0)	270.1 (363.7)	0.6 (2.6)
CT9 – Non-gradient pattern	29.1 (1.8)	297.1 (408.4)	−0.2 (2.4)

3.7. CT7: North-eastern flow

Azores high extended over the Atlantic and Western Europe, causing north to east winds over the area. Lightning activity is concentrated over the southernmost chains of the Pyrenees, showing high amounts of lightning flashes in a large area. In this situation, the Pyrenees have an important orographic effect, triggering a low-pressure centre on the leeward side over Catalonia and Andorra (orographic dipole effect), where important convergence zones can be generated and further initiate convective processes (Bessemoulin et al., 1993). In addition to this orographic effect, the diurnal solar heating effect reinforces thunderstorm activity at the 12 h and 18 h UTC periods over the southern area of the Pyrenees range. Concerning Andorra, the area is affected by low lightning activity. This pattern represents 22% of the 6-h periods, and is also the most frequent one in summer, including most of the lightning activity.

3.8. CT8: Azores anticyclone

This centre of action spreads over the study area, and northerly winds blow over the Pyrenees. The orographic dipole effect is also present in this type, but a westerly to north-westerly flow at 500 hPa reduces thunderstorm activity over the Pyrenees area (CT with the lowest values over Andorra). It is well-known that the convergence is concentrated over the north-eastern area of Catalonia, represented by a small maximum on the lightning distribution maps. The occurrence frequencies maximum appears in summer and during the evening-night time period.

3.9. CT9: Non-gradient pattern

This type is very typical over the Mediterranean (in Catalan *Pantà Baromètric*, i.e. barometric swamp), showing very weak SLP gradients over the western Mediterranean. Its distinct daily cycle is associated with diurnal variations in solar radiation with maxima between 12 and 18 h. The seasonal maximum is concentrated in late spring and the beginning of summer. The spatial lightning distribution for this type is quite similar to Type 7, where convection and thunderstorms are located in mountainous regions (southern area of Pyrenees range). Furthermore, a secondary maximum is located in the inland areas of the southern half of Catalonia. Moderate values are observed over Andorra, mainly in its southern half.

3.10. Circulation pattern persistence

We analyzed the transitions between circulation types in two consecutive 6-h periods (2CT) in order to detect relationships between CTs and to analyse their persistence. A total of 43% of the 6-h samples used in the classification of circulation types are followed by another important lightning event, while 57% are "solitaire" events. As can be seen in Fig. 3d, of all the possible 2CT combinations (CT A–CT B), the highest frequencies occur in sequences of the same CT. The most frequent sequence is CT7–CT7, presenting 15% of the cases, followed by CT1–CT1 (11%). The reason for these high percentages is persistent anticyclonic configurations, which are characteristic of both CTs. For instance, a 5-day episode for CT1 appeared during September 2006. Moreover, the low occurrence of the CT5–CT5 sequence (Iberian thermal low) can be attributed to the patent midday nature of this thermal pattern; which relatively increases the frequency of the CT5–CT7 sequence, because the thermal low over Iberia disappears in the afternoon-evening. The secondary maximum for CT6–CT3 and CT9–CT3 sequences is noteworthy. Both cases show similar evolutions, present a weak SLP gradient over the study area and are followed by the formation of a Mediterranean low. The first sequence is known in terms of weather forecasting and synoptic climatology over the study area. In summer the contact of cold air, associated with a frontal system (CT6), with the Mediterranean air mass favours the generation of cyclogenesis (CT3) and triggers atmospheric instability. This is not the case for the CT9–CT3 sequence, in which the results obtained can likely be conditioned by the size of the dataset for the period analyzed. It is also interesting to analyse when these 2CT sequences occur. A total of 54% of the 2CT combinations start at 12 h, indicating that the majority of thunderstorms starting in the early afternoon extend their lifetime until night. From the 2CT starting at noon, 50% do so with CT2, CT5 and CT7 configurations and thunderstorm formation is therefore mainly related to the diurnal radiation cycle.

3.11. Atmospheric indices characterizing circulation types

We calculated some instability indices, such as temperature difference between 850 and 500 hPa (TD850-500), Convective Available Potential Energy (CAPE) and Lifted Index (LI), for all the 6-h periods and the 7 cells corresponding to Catalonia and Andorra in the NCEP FNL data (Table 1).

The highest mean values of TD850-500 obtained (CT9 29.1 °C and CT5 29.0 °C) correspond to circulations types in which convection does not rely on dynamic factors, but rather is due to thermal contrasts between low and middle levels. These two types also exhibit lower CAPE values (231.2 J/kg and 297.1 J/kg respectively), indicating the lack of dynamic factors in convection triggering under these CTs. Furthermore, atmospheric instability (higher CAPE, lower LI) is highest for Westerly flow (CT4: CAPE 476.9 J/kg and LI −1.1), followed by cold front (CT6: CAPE 378.6 J/kg and LI −0.7) and Easterly flow (CT1: CAPE 365.7 J/kg and LI −0.7), which indicates that convection under these regimes is dominated mainly by dynamic factors; thus, values of TD850-500 in CT1 are quite low (27.7 °C). Overall, we have observed that in CT's for which thermal dynamics constitutes the most significant factor (i.e. CT5, CT9) the values of TD850-500 from June to August fluctuate at around 29 °C (with ±2 °C deviation), whereas the remaining CTs present lower values, close to 27 °C (±2, 2 °C deviation).

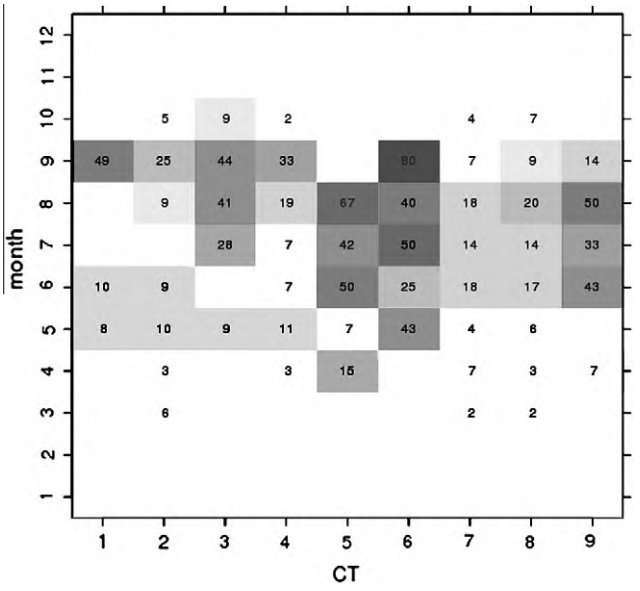

Fig. 5. Monthly frequencies of occurrence (%) of over 200 CG flashes for 6-h SLP fields from the 2003–2007 period similar (exhibiting a pattern correlation value higher than 0.8) to one of the nine centroids from Fig. 2.

Finally, it is worth pointing out that we observed similarities in the spatial distribution of lightning and the Atmospheric Instability Indices. For instance, the Easterly flow (CT1) shows higher lightning activity in the south (see Fig. 4), where the values of CAPE are higher in this CT (660.2 J/kg). Also, in the North-eastern flow (CT7), the CAPE and LI mean values (345.4 J/kg and −0.5 respectively) indicate that atmospheric instability is greater in the northern half of the study area, where lightning activity has proven to be the most intense. In CTs like the Easterly flow (CT1) and the Mediterranean low (CT3), convection is concentrated along the south coast of Catalonia, as a result of dynamic factors such as eastern advection or the presence of lows.

3.12. Frequencies of occurrence of enhanced lightning activity for SLP fields similar to CT centroids

From results presented to date, it is difficult to establish how typical the SLP-composites (centroids) representing the CTs are for periods of enhanced lightning activity, i.e. the frequency with which synoptic situations similar to one of the centroids are related to more than 200 flashes during the corresponding 6-h period. Thus, we performed an additional analysis in order to determine how often SLP fields resembling one of the lightning cluster centroids are related to enhanced lightning activity (over 200 flashes during the respective 6-h period). Using the same dataset as for the circulation type classification, for each of the nine centroids derived from the classification of 6-h SLP fields related to lightning activity (see Fig. 2), we calculated the pattern correlations (Pearson correlation coefficients) between the centroid and any 6-h SLP field from the whole sample (7304 cases). All cases (with and without enhanced lightning activity) were then assigned to the most similar of the nine CT centroids in terms of pattern correlation exceeding a value of 0.8. Following this approach, 50% of all lightning events and 39% of all non-lightning events can be assigned to the CT centroids derived from the classification of 6-h periods presenting lightning activity. This appears to indicate that not all synoptic situations related to lightning activity are clearly represented by the centroids shown in Fig. 2 and that these centroids (unsurprisingly) do not reflect the whole range of synoptic situations realized during the whole period from 2003 to 2007. Subsequently, for each centroid the frequency of occurrence of enhanced lightning activity – for SLP configurations similar to the centroid – was calculated as the fraction of lightning cases assigned to the respective centroid. Fig. 5, which shows the resulting monthly frequencies of occurrence of enhanced lightning activity for the nine centroids from Fig. 2, reveals distinctly high frequencies of occurrence (>40%), especially for SLP configurations similar to the centroids of the low-gradient types CT5 (June–August) and CT9 (June and August), the cold-front type CT6 (May and July–September), the Mediterranean low represented by CT3 (August, September) and the Easterly flow situation from CT1 (September). However, it should be mentioned that some of the distinctly high relative frequencies of occurrence values in Fig. 5 (CT6 in September, CT5 in August and CT9 in August) rely on very low numbers of cases assigned to the respective centroids.

4. Conclusions

Based on 6-h periods of substantial lightning activity (over 200 flashes) over Catalonia and the Principality of Andorra from 2003 to 2007, we obtained a nine-type circulation catalogue. The classification method used in this study is based on an S-mode Principal Component Analysis with the "extreme scores" variant for clustering all the cases.

Clear differences can be found on observing the average SLP fields obtained for each type, and these differences become more distinct when other parameters such as frequency (monthly and 6-h), spatial distribution of flashes and pattern persistence are analyzed. Consequently, it can be concluded that three main groups of patterns are obtained from the scale/dynamical origin point of view: those related to synoptic dynamics (CT1, CT3, CT4, CT6), i.e. resulting from the location of the centres of action and the pass of frontal systems; those related to mesoscale dynamics (CT2, CT7, CT8), i.e. the formation of mesoscale systems as a consequence of orographic effect (mainly the Pyrenees); those related to thermal dynamics associated with solar heating (CT5, CT9), i.e. as a consequence of the effect of coastal and mountain breezes triggering instability.

It is also interesting to highlight the analysis of the persistence of the types obtained, which reinforces the consistency of the results. It shows how types characterized by anticyclonic configurations are more likely to persist, especially in mid summer, while thermal patterns usually show short sequences and are concentrated between midday and evening.

Furthermore, the use of atmospheric instability indices related to each pattern did not provide the results expected with regard to improving the characterization of the types obtained. However, the results of TD850-500 (combined with other factors like orography or meso scale flows) could help to improve weather forecasting during summer months, especially when CT associated with solar heating are present (CT5 and CT9).

Nonetheless, there is some similarity between the spatial distribution of the indices calculated and the location of lightning activity, particularly in the types related to dynamical factors. We will perform a painstaking analysis in this sense in the near future using radiosonde data over the study area, which will enable us to improve the results in terms of mean and deviation of CAPE and LI values obtained with the FNL data.

Finally, the results obtained from the monthly frequencies of occurrence of substantial lightning activity according to the SLP fields can be considered to be relevant with respect to lightning forecast issues. It should not be forgotten that some of the distinctly high occurrence frequencies are estimated on the basis of a very low number of cases. It can, however, be concluded that representatives of the group of CTs reflecting synoptic dynamics (CT1,

CT3, CT6), as well CTs characterized by weak gradients (CT5 and CT9) exhibit a close relationship with enhanced lightning activity, at least during some months between June and September. To the contrary, all CTs reflecting mesoscale dynamics (CT2, CT7 and CT8) generally show lower values of frequencies of occurrence.

To conclude, our classification method is useful for the identification of relevant circulation types related to non-continuous events such as lightning activity, and for deriving valuable climatological and meteorological information. The procedure presented in our paper could also be applied to other phenomena, including extreme events, thus helping to increase our knowledge of their genesis mechanisms, and to create "rules-of-thumb" for weather forecasters.

Acknowledgments

The authors wish to thank Thomas Krennert of the Central Institute for Meteorology and Geodynamics (ZAMG), Austria, Oriol Argemí and Joan Bech from the Meteorological Service of Catalonia (SMC) and Javier Martín-Vide from the University of Barcelona (2009 SGR 443 GRUP DE CLIMATOLOGÍA) for their technical support. We would also like to thank the two reviewers for their useful comments, which were of considerable help in improving the text.

References

Action Cost 733, February 2009. Harmonisation and Applications of Weather Types Classifications for European Regions. <http://www.cost733.org>.

Barry, R.G., Carleton, A.M., 2001. Synoptic and Dynamic Climatology. Routledge, London.

Bessemoulin, P., Bougeault, P., Genovés, A., Jansà, A., Puech, D. 1993. Mountain pressure drag during PYREX. Beiträge zur Physik de Atmosphäre 66, 305–325..

Birkeland, K.W., Mock, C.J., Shinker, J.J., 2001. Avalanche extremes and atmospheric circulation patterns. Annals of Glaciology 32, 135–140.

DOC/NOAA/NWS/NCEP, 2000. NCEP FNL Global Tropospheric Analyses, 1x1, daily 1999Jul30- present, updated daily. Published by the CISL Data Support Section at the National Centre for Atmospheric Research, Boulder, CO (ds083.2).

Esteban, P., Jones, P.D., Martín-Vide, J., Mases, M., 2005. Atmospheric circulation patterns related to heavy snowfall days in Andorra, Pyrenees. International Journal of Climatology 25, 319–329.

Esteban, P., Martín-Vide, J., Mases, M., 2006. Daily atmospheric circulation catalogue for Western Europe using multivariate techniques. International Journal of Climatology 26, 1501–1515.

Esteban, P., Ninyerola, M., Prohom, M., 2009. Spatial modelling of air temperature and precipitation for Andorra (Pyrenees) from daily circulation patterns. Theoretical and Applied Climatology 96, 43–56.

Hagen, M., Finke, U., 1999. Motion characteristics of thunderstorms in southern Germany. Meteorological Applications 6, 227–239.

Huth, R., Beck, C., Philipp, A., Demuzere, M., Ustrnul, Z., Cahynová, M., Kyselý, J., Tveito, O.E., 2008. Classification of atmospheric circulation patterns – recent advances and applications. Annals of the New York Academy of Sciences 1146, 105–152. doi:10/1196annals.1446.019.

Jansà, J.M., 1959. La masa de aire mediterránea. Revista de Geofísica 18, 35–50.

Jenkinson, A.F., Collison, F.P., 1977. An initial climatology of gales over the North Sea. Synoptic Climatology Branch Memorandum No.62, Meteorological Office, Bracknell.

Kostopoulou, E., 2003. The relationships between atmospheric circulation patterns and surface climatic elements in the eastern Mediterranean. PhD. Thesis, University of East Anglia, Norwich.

Lericos, T.P., Fuelberg, H.E., Watson, A.I., Holle, R.L., 2002. Warm season lightning distributions over the Florida Peninsula as related to synoptic patterns. Weather and Forecasting 17, 83–98.

Llasat, M.C., Puigcerver, M., 1994. Meteorological factors associated with floods in the north-eastern part of the Iberian Peninsula. Natural Hazards 9, 81–93.

López, R. E., Holle, R. L., 1987. The distribution of lightning as a function of low-level wind flow in central Florida. NOAA Tech. Memo. ERL ESG-28, National Severe Storms Laboratory, Norman, OK, 43 pp.

Martín-Vide, J, 2005. Los mapas del tiempo. Mataró: Davinci. 219pp.

Philipp, A., Bartholy, J., Beck, C., Erpicum, M., Esteban, P., Fettweis, X., Huth, R., James, P., Jourdain, S., Kreienkamp, F., Krennert, T., Lykoudis, S., Michalides, S., Pianko, K., Post, P., Rassilla Álvarez, D., Spekat, A., Tymvios, F.S., 2010. COST 733CAT – a database of weather and circulation type classifications. Physics and Chemistry of the Earth 35, 360–373.

Pineda, N., Montanyà, J., 2009. Lightning detection in Spain: the particular case of Catalonia. In: Betz, H.D., Schumann, U., Laroche, P. (Eds.), Lightning: Principles, Instruments and Applications: Review of Modern Lightning Research. Springer, p. 641.

Reap, R.M., 1994. Analysis and prediction of lightning strike distributions associated with synoptic map types over Florida. Monthly Weather Review 122, 1698–1715.

Richard, P., Lojou, J.Y., 1996. Assessment of application of storm cell electrical activity monitoring to intense precipitation forecast. In: 10th Int. Conf. on Atmospheric Electricity, Osaka, Japan, pp. 284–287.

Richman, M.B., 1986. Rotation of principal components. Journal of Climatology 6, 293–335.

Tait, A.B., Fitzharris, B.B., 1998. Relationship between New Zealand rainfall and south-west Pacific pressure patterns. International Journal of Climatology 18, 407–424.

Tomás, C., de Pablo, F., Rivas Soriano, L., 2004. Circulation weather types and cloud-to-ground flash density over the Iberian Peninsula. International Journal of Climatology 24 (1), 109–123.

Yarnal, B., 1993. Synoptic Climatology in Environmental Analysis. Belhaven Press, London.